I&EC research
Industrial & Engineering Chemistry Research

Subscriber access provided by LAURENTIAN UNIV

Article

Enhancing a Smelter Off-Gas System Using a Plant-Wide Control Design

Antonio C. B. de Araujo, and Helen Shang

Ind. Eng. Chem. Res., **2009**, 48 (6), 3004-3013• DOI: 10.1021/ie800254s • Publication Date (Web): 12 February 2009

Downloaded from http://pubs.acs.org on March 25, 2009

More About This Article

Additional resources and features associated with this article are available within the HTML version:

- Supporting Information
- Access to high resolution figures
- Links to articles and content related to this article
- Copyright permission to reproduce figures and/or text from this article

View the Full Text HTML

ACS Publications
High quality. High impact.

Industrial & Engineering Chemistry Research is published by the American Chemical Society. 1155 Sixteenth Street N.W., Washington, DC 20036

Enhancing a Smelter Off-Gas System Using a Plant-Wide Control Design

Antonio C. B. de Araujo and Helen Shang*

School of Engineering, Laurentian University, Sudbury, Ontario, Canada

An off-gas treatment system is a vital component of smelter roaster processes as it ensures operation is in accordance with environmental regulations in terms of hazardous emissions. It is, therefore, paramount that a well-designed control structure be incorporated into the system. Analysis of the off-gas treatment processes for a roaster using a systematic control design procedure to provide the necessary verification to current industrial practices for controlling these processes was carried out. We approached this by conducting a top-down (steady-state) analysis based on an available nonlinear model of the process. The results provide insight into, and potential improvement of, the control of the off-gas system. Through designing the bottom-up structure, a feedback control structure was developed to give robust and effective control in terms of disturbance rejection capabilities. The proposed control structure provides for improved performance in an easy form to implement.

1. Introduction

In nickel production, sulfide ores are usually roasted for sulfur and/or iron removal before smelting in the furnace. Roasting of sulfide concentrates generates off-gases laden with sulfur dioxide (SO_2).[1] The environmental damage and harmful impacts of SO_2 emissions from the smelters have been extensively studied and reported.[2,3] A great amount of investment and effort have been made on sulfur dioxide emission reduction, and significant environmental improvement has been achieved.[4,5] Many smelting operations, however, still rely on very tall stacks and windy weather to reduce on-site concentration of sulfur dioxide, and will struggle to satisfy environmental regulations as the limit of SO_2 atmospheric emissions becomes tighter. The SO_2 atmospheric emissions issue may, therefore, become the "bottleneck" of nickel productions. With increasingly stringent environmental regulations, continued effort on SO_2 emission reduction is required to ensure a desirable working environment and the satisfactory operation of nickel smelters.

A large amount of work has been reported in modeling the smelting processes, especially in modeling of smelting furnaces of various types.[6,7] Despite its environmental significance, research on modeling and control issues of smelter off-gas systems has, however, been limited.[8,9] Bekker et al. carried out an extensive modeling on an electric arc furnace off-gas process tackling hazardous carbon monoxide, and a model predictive control approach was developed.[10,11] Roaster off-gas systems that deal with SO_2 emissions are frequently emphasized in some industrial presentations.[4,5,12] A detailed study on the dynamic model of an industrial roaster off-gas system using fundamental principles of mass continuity, momentum, and energy conservation was performed by Shang et al.[13] This paper uses the developed model to design a suitable control structure for this important industrial system. It represents a fundamental study of an industrial roaster off-gas system in a nickel smelter, the results of which can be applicable to other roaster off-gas systems as well as potentially applicable for gas cleaning systems in other industries.

Reduction of SO_2 emission to the atmosphere may be conservatively achieved by maintaining a slight negative pressure in the off-gas systems and thus minimizing SO_2 out-leakage. Pressure control in roaster off-gas systems is not only critical for environmental purposes, but can also help maintain a stable smelter operation.

This paper aims at designing a control structure for such plants to ensure operational objectives are achieved at the lowest possible cost. For this purpose, a systematic approach is paramount and we have based the work on the well-established design procedure proposed by Skogestad.[14]

2. Process Description

The roaster off-gas system at Xstrata Nickel's Sudbury Smelter (Figure 1) represents a good example of off-gas cleaning systems used in metallurgical industry. The copper−nickel slurry from mineral processing plants is fed to a fluidized bed roaster and "burned" with the aid of the fluidizing air. This exothermal reaction continues without the need for adding additional heating resources. The reaction

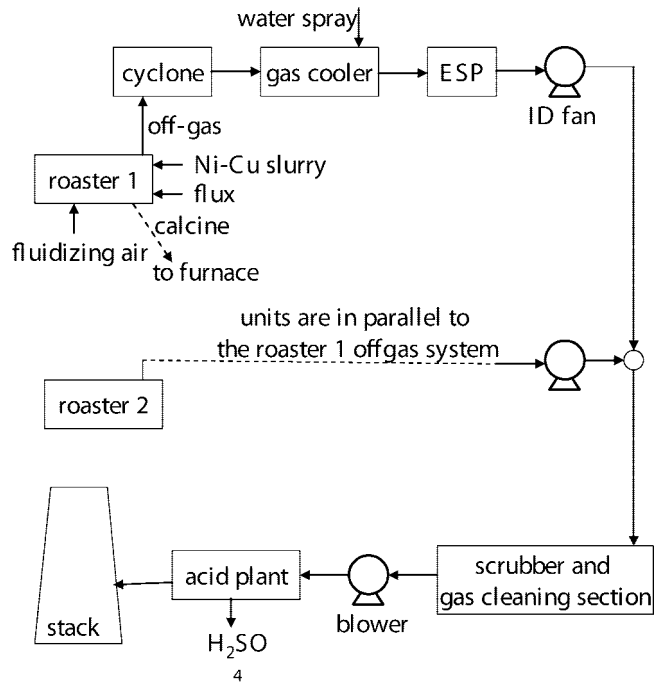

Figure 1. Schematic diagram of an industrial roaster off-gas system.

* To whom correspondence should be addressed. E-mail: hshang@laurentian.ca. Address: School of Engineering, Sudbury, ON, Canada P3E 2C6.

10.1021/ie800254s CCC: $40.75 © 2009 American Chemical Society
Published on Web 02/12/2009

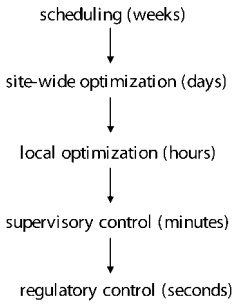

Figure 2. Typical control hierarchy in a chemical plant.

generates a large amount of SO_2 which, along with the remaining fluidizing air, water vapor from the slurry, and the flux, constitute the roaster off-gas.[15] This off-gas, carrying finer particles of roasted concentrate or calcine, is extracted through one or two ports at the top of the roaster.

The off-gas from the roaster enters a pair of primary cyclones and the fine solid calcine is removed from the gas. The off-gas is then cooled from 650−680 to 300−350 °C using an atomized water spray. The cooled gas passes an electro-static precipitator (ESP). On the discharge side of the ESP, the roaster off-gas induced draft (ID) fans draw the gas through the gas cleaning train and discharge the dust free gas into a flue connected to the acid plant. The off-gases exiting the ID fans on the two roaster off-gas lines are combined and enter the acid plant scrubber and the gas cleaning section for cooling, drying, and further cleaning. The acid plant blower is used to transport the dried dust free gas to the wet acid plant, where sulfur dioxide is converted to sulfuric acid.

To maintain a desirable working environment, it is important to minimize off-gas out-leakage, which can be achieved by keeping stable negative pressure in the unit operations before the wet acid plant. A well designed control system using the SO_2 blower and the two ID fans as the manipulated variables is necessary to control the off-gas pressure at the negative setpoints without high energy cost. On the basis of the dynamic model derived in Shang et al.,[13] a plant-wide control structure design was applied to the off-gas system as described in the following sections.

3. A Plantwide Control Structure Design Procedure

A control system is usually divided into several layers, separated by time scale (Figure 2). The layers are linked by the controlled variables, whereby the set points are computed by the upper layer and implemented by the lower layer. Control structure design, also known as plantwide control, deals with the structural decisions that must be made to design a control structure. A systematic procedure for this purpose has been developed by Skogestad[14] and successfully implemented in the well-known test-bed HDA plant.[16,17]

The plant-wide control design procedure consists of top-down analysis and bottom-up design. The top-down analysis includes definition of operational objectives, degrees of freedom, and selection of primary controlled variables (y_1) and is performed with the following steps.

Step 1. Definition of operational objectives: identifying operational constraints and a scalar cost function J to be minimized.

Step 2. Manipulated variables u and degrees of freedom: identifying dynamic and steady-state degrees of freedom (DOF).

Table 1. List of Manipulable Variables

	manipulated variable	status in this work
W_{in1}	inlet gas flow rate of roaster 1 freeboard [kg/s]	steady state
W_{in2}	inlet gas flow rate of roaster 2 freeboard [kg/s]	steady state
W_{w1}	water to gas cooler 1 [kg/s]	steady state
W_{w2}	water to gas cooler 2 [kg/s]	steady state
Z_{F1}	ID fan 1 vane position [%]	steady state
Z_{F2}	ID fan 2 vane position [%]	steady state
Z_B	blower vane position [%]	steady state

Table 2. Selected Candidate Controlled Variables

	candidate controlled variable
P_{R1}	roaster 1 freeboard pressure [Pa]
P_{C1}	cyclone 1 pressure [Pa]
P_{G1}	gas cooler 1 pressure [Pa]
P_{E1}	electrostatic precipitator (ESP) 1 pressure [Pa]
P_{F1}	ID fan 1 outlet pressure [Pa]
P_{R2}	roaster 2 freeboard pressure [Pa]
P_{C2}	cyclone 2 pressure [Pa]
P_{G2}	gas cooler 2 pressure [Pa]
P_{E2}	electrostatic precipitator (ESP) 2 pressure [Pa]
P_{F2}	ID fan 2 outlet pressure [Pa]
P_{Si}	scrubber inlet pressure [Pa]
P_S	gas cleaning section pressure [Pa]
P_B	blower outlet pressure [Pa]
T_{G1}	gas cooler 1 temperature [K]
T_{G2}	gas cooler 2 temperature [K]
Z_{F1}	ID fan 1 vane position [%]
Z_{F2}	ID fan 2 vane position [%]
Z_B	blower vane position [%]

Step 3. Selection of primary controlled variables: controlling active constraints and achieving self-optimizing control.

Step 4. Primary controlled variables: deciding where the production rate should be set.

The bottom-up design of the control system starts with the stabilizing control layer and includes the following steps.

Step 5. Design of the regulatory control layer: "stabilizing" the plant using low-complexity controller (single-loop PID controllers) such that (a) the plant does not drift too far away from its nominal operating point and (b) the supervisory layer (or the operators) can handle the effect of disturbances on the primary outputs.

Step 6. Design of the supervisory control layer: identify dynamic and steady-state degrees of freedom (DOF).

Step 7. Design of the optimization layer (RTO): identifying active constraints and compute optimal set points for controlled variables.

Step 8. Validation: nonlinear simulation of the plant.

Detailed description of these steps can be found in the work by Skogestad.[14]

4. Top-down (Steady-State) Analysis

This section presents the application of Steps 1−4, as described in section 3, to the nickel smelter off-gas system starting with the degree of freedom analysis. Note that, in the top-down analysis, a nonlinear steady-state process model is required and that analysis is based on steady-state conditions.

4.1. Degree of Freedom Analysis. Tables 1−3 list 7 manipulated variables, 18 candidate measurements, and 17 disturbances, respectively. In Tables 1 and 2, Z_{F1}, Z_{F2} and Z_B are listed as both the manupulated variables (MV) and controlled variables (CVs). This is because, in the self-optimizing technology, MVs are "appointed" as candidate CVs with the aim of trying to keep them fixed, at least at steady state for minimal manipulation handling. The 7 manipulated variables correspond

Table 3. Disturbances to the Process

	disturbance description	nominal	disturbance (Δ)
D1	inlet gas flow rate of roaster 1 and 2 [kg/s]	18 + 18	−2 × 1.8 (−10%)
D2	inlet gas flow rate of roaster 1 and 2 [kg/s]	18 + 18	+2 × 1.8 (+10%)
D3	inlet gas flow rate of roaster 1 [kg/s]	18	−1.8 (−10%)
D4	inlet gas flow rate of roaster 1 [kg/s]	18	+1.8 (+10%)
D5	inlet gas flow rate of roaster 2 [kg/s]	18	−1.8 (−10%)
D6	inlet gas flow rate of roaster 2 [kg/s]	18	+1.8 (+10%)
D7	effective in-leakage area in roaster 1 [m^2]	0.0120	+0.0060 (+50%)
D8	effective in-leakage area in roaster 1 to ESP 1 inlet [m^2]	0.0190	+0.0095 (+50%)
D9	effective in-leakage area in ESP 1 [m^2]	0.0590	+0.0295 (+50%)
D10	effective in-leakage area in roaster 2 [m^2]	0.0110	+0.0055 (+50%)
D11	effective in-leakage area in roaster 2 to ESP 2 inlet [m^2]	0.0530	+0.0265 (+50%)
D12	effective in-leakage area in ESP 2 [m^2]	0.0350	+0.0175 (+50%)
D13	effective in-leakage area from ID fan duct to scrubber inlet [m^2]	0.0820	+0.0410 (+50%)
D14	effective in-leakage area in gas cleaning section [m^2]	0.1300	+0.0650 (+50%)
D15	effective in-leakage area in blower inlet [m^2]	0.0220	+0.0110 (+50%)
D16	room temperature [K]	273	−30
D17	room temperature [K]	273	+30

to 7 dynamic degrees of freedom and, equivalently, 7 degrees of freedom at steady state because there are no liquid levels with economic impact on the process that need to be controlled. When the two gas flow rates of the roasters are not available for control, 5 degrees of freedom are available.

With 7 degrees of freedom and 18 candidate controlled variables, there are $\binom{18}{7} = 18!/(7!11!) = 31824$ control structures. Even if one considers that the two gas flow rates of the roasters are not available for control, there is still $\binom{18}{5} = 18!/(5!13!) = 8568$ possible combinations. Clearly, analysis of all the combinations is rather intractable. To avoid this combinatorial explosion, the active constraints which should be controlled to achieve optimal operation need to be determined.[18]

4.2. Definition of Optimal Operation. The objective is to use as little power as possible in the ID fans and blower subject to avoiding gas out-leakage. Therefore, the following cost function based on the useful power consumption of a fan,[19] J, is to be minimized:

$$J = \frac{pK}{\varepsilon\rho C_q}[(P_{F1} - P_{E1})W_{F1} + (P_{F2} - P_{E2})W_{F2} + (P_B - P_S)W_B] \quad (1)$$

where p is the price of electricity; K is a coefficient that accounts for the compressibility of the gas (assumed constant); ε is the fan efficiency (assumed the same for all fans); ρ is the gas density (assumed constant throughout); C_q is a constant that adjusts the dimension of the units used; P_{F1} and P_{F2} are the ID fans 1 and 2 discharge pressures; P_{E1} and P_{E2} are the electrostatic precipitator ESP 1 and 2 pressures; P_S is the blower inlet pressure; P_B is the blower discharge pressure; W_{F1} and W_{F2} are the mass flow rates from ID fans 1 and 2; and W_B is the mass flow rate exiting the blower. Note that cooling water pumping cost also constitutes part of power comsumption. When more cooling water is pumped, the off-gas flow rate and the power cost on the ID fans and blowers increase. The effect of water pumping cost is, therefore, implicitly included in the cost function. However, with fixed roaster feed rate, the water pumping cost will not vary much and in this case the water pumping cost is not explicitly included in the cost function 1.

By factoring out the constants in 1, the cost function can be defined as

$$J' = \frac{\varepsilon\rho C_q}{pK}J = (P_{F1} - P_{E1})W_{F1} + (P_{F2} - P_{E2})W_{F2} + (P_B - P_S)W_B \quad (2)$$

The constraints to which the process is subjected are listed in Table 4. Steady-state bounds mean the constraints cannot be violated when the system operates under steady-state conditions. On the other hand, dynamic bounds refer to a short-term situation in which the static bounds can be violated dynamically, provided they always return to their optimal setpoints. All the pressure constraints are to avoid leakage to the atmosphere and are gauge measurements. It is assumed that the fans have enough available power and, therefore, no constraints are imposed on these variables. Water supply to the gas coolers is also assumed unconstrained.

Table 4. Constraints to the Process

	constraint description	bound
P_{R1}	roaster 1 freeboard pressure [Pa]	<0
P_{R2}	roaster 2 freeboard pressure [Pa]	<0
P_{C1}	cyclone 1 pressure [Pa]	<0
P_{C2}	cyclone 2 pressure [Pa]	<0
P_{G1}	gas cooler 1 pressure [Pa]	<0
P_{G2}	gas cooler 2 pressure [Pa]	<0
T_{G1}	gas cooler 1 temperature [K]	<643
T_{G2}	gas cooler 2 temperature [K]	<643
W_{w1}	water to gas cooler 1 [kg/s]	>0
W_{w2}	water to gas cooler 2 [kg/s]	>0
P_{E1}	electro-static precipitator (ESP) 1 pressure [Pa]	<0
P_{E2}	electro-static precipitator (ESP) 2 pressure [Pa]	<0
P_{F1}	ID fan 1 outlet pressure [Pa]	<0
P_{F2}	ID fan 2 outlet pressure [Pa]	<0
Z_{F1}	ID fan 1 vane position [%]	[0 100]
Z_{F2}	ID fan 2 vane position [%]	[0 100]
P_{Sis}	Scrubber inlet pressure [Pa]	<0
P_S	gas cleaning section pressure [Pa]	<0
Z_B	blower vane position [%]	[0 100]

Table 3 lists 17 disturbances considered in analysis and optimization. They include changes in the feed flow to the process and in the effective in-leakage area of various units.

4.3. Optimization. On the basis of the model in Shang et al.,[13] optimization is performed for each condition imposed by the selected disturbances (Table 3) subject to the constraints defined in Table 4. In this subsection, the inlet gas flow rates to the roaster freeboards (W_{in1} and W_{in2}) are assumed fixed. The case that they are treated as degrees of freedom (production rate/throughput analysis) is discussed in the next subsection.

The in-built Matlab subroutine "fmincon.m" was used for optimization. The results indicate that 4 constraints are always active, namely, P_{R1} (upper bound), T_{G1} (upper bound), P_{R2} (upper bound), and T_{G2} (upper bound). To prevent gas outleakage, it is necessary to reduce the upper bound on P_{R1}, P_{R2}, P_{F1}, and P_{F2}. We followed the results obtained by Shang *et al.*[20] and set P_{R1}, $P_{R2} < -1000$ Pa and P_{F1} $P_{F2} < -200$ Pa as the new constraints. Table 5 and Figure 3 show the optimization results with the modified constraints. Similarly, P_{R1}, T_{R1}, P_{R2}, and T_{R2}

Table 5. Effect of Disturbances on Optimal Values for Related Variables

variable	unit	nominal	D1	D2	D3	D4	D5	D6	D7	D8	D9	D10	D11	D12	D13	D14	D15	D16	D17
P_{R1}	Pa	−1000	−1000	−1000	−1000	−1000	−1000	−1000	−1000	−1000	−1000	−1000	−1000	−1000	−1000	−1000	−1000	−1000	−1000
P_{C1}	Pa	−2664	−2349	−3005	−2349	−3005	−2661	−2661	−2682	−2661	−2661	−2661	−2661	−2661	−2661	−2661	−2661	−2661	−2661
P_{G1}	Pa	−3329	−2889	−3807	−2889	−3807	−3325	−3325	−3354	−3325	−3326	−3326	−3326	−3326	−3326	−3326	−3326	−3326	−3326
T_{G1}	K	643	643	643	643	643	643	643	643	643	643	643	643	643	643	643	643	643	643
P_{E1}	Pa	−4228	−3620	−4893	−3620	−4893	−4225	−4225	−4262	−4249	−4249	−4225	−4225	−4225	−4225	−4225	−4225	−4225	−4199
P_{Si}	Pa	−755	−654	−866	−755	−864	−752	−866	−757	−766	−808	−760	−793	−788	−755	−755	−755	−740	−772
P_S	Pa	−10441	−9419	−11476	−9990	−11020	−9987	−11024	−10465	−10510	−10733	−10467	−10643	−10618	−10576	−10441	−10441	−10294	−10601
P_{R2}	Pa	−1000	−1000	−1000	−1000	−1000	−1000	−1000	−1000	−1000	−1000	−1000	−1000	−1000	−1000	−1000	−1000	−1000	−1000
P_{C2}	Pa	−2657	−2346	−3001	−2657	−2657	−2346	−3001	−2657	−2657	−2658	−2677	−2658	−2658	−2658	−2658	−2658	−2658	−2658
P_{G2}	Pa	−3321	−2885	−3802	−3321	−3321	−2885	−3802	−3321	−3321	−3321	−3348	−3321	−3321	−3321	−3321	−3321	−3321	−3321
T_{G2}	K	643	643	643	643	643	643	643	643	643	643	643	643	643	643	643	643	643	643
P_{E2}	Pa	−4306	−3688	−4988	−4306	−4306	−3688	−4988	−4306	−4306	−4306	−4341	−4376	−4306	−4306	−4306	−4306	−4277	−4337
Z_{F1}	%	63.9	54.8	73.9	52.8	73.9	63.9	61.6	64.5	64	62.3	63.8	63.1	63.2	63.9	63.9	63.9	63.8	64
Z_{F2}	%	65.5	56.1	75.7	65.5	63.3	54.2	75.7	65.4	65.2	64.4	66	65.7	64.5	65.5	65.5	65.5	65.3	65.6
Z_B	%	45.7	41.5	49.9	43.7	47.9	43.7	47.9	45.8	45.9	46.8	45.8	46.4	46.3	46.23	47.32	46.19	45.05	46.3
P_{F1}	Pa	−203	−202	−203	−304	−200	−200	−314	−200	−200	−200	−207	−240	−236	−203	−203	−203	−202	−203
P_{F2}	Pa	−200	−200	−200	−200	−309	−299	−200	−203	−211	−253	−200	−200	−200	−200	−200	−200	−200	−200
W_{w1}	kg/s	2.32	2.09	2.56	2.09	2.56	2.32	2.32	2.31	2.27	2.32	2.32	2.32	2.32	2.32	2.32	2.32	2.01	2.66
W_{w2}	kg/s	2.15	1.92	2.37	2.15	2.15	1.92	2.37	2.15	2.15	2.15	2.13	2.01	2.15	2.15	2.15	2.15	1.83	2.49
cost	−	1.28	1.05	1.54	1.17	1.41	1.17	1.41	1.29	1.3	1.34	1.29	1.32	1.32	1.31	1.41	1.31	1.25	1.32

Loss Caused by Disturbances for Alternative Sets of Controlled Variables[a]

variable	D1	D2	D3	D4	D5	D6	D7	D10	D16	D17
P_{C1}	inf	inf	inf	inf	0	0	0	0	0	
P_{G1}	inf	inf	inf	inf	0	0	inf	0	0	0
P_{E1}	inf	inf	inf	inf	0	0	inf	0	inf	inf
P_{F1}	0	inf	inf	0.0001	0.0002	inf	0.0001	inf	0	inf
P_{C2}	inf	inf	0	0	inf	inf	0	inf	0	0
P_{G2}	inf	inf	0	0	inf	inf	0	inf	0	0
P_{E2}	inf	inf	0	0	inf	inf	0	inf	inf	inf
P_{F2}	0	0	0	inf	inf	0	inf	0	0	0
P_{Si}	0.0044	inf	0	inf	0.0002	inf	inf	inf	0.0007	inf
P_S	0.0336	inf	0.0157	inf	0.0158	inf	inf	inf	0.0055	inf
P_B	inf	inf	0.0746	inf	0.0747	inf	inf	inf	0.0223	inf
Z_{F1}	inf	0.0206	inf	0.0203	0.0002	inf	0.0014	inf	inf	0.0001
Z_{F2}	inf	0.0212	0	inf	inf	0.0207	inf	0.0012	inf	0.0002
Z_B	0.0530	inf	0.0263	inf	0.0264	inf	inf	inf	0.0088	inf

[a] inf means infeasible operation.

Table 6. Robust Loss Calculations for Alternative Sets of Controlled Variables

variable	optimum set point	robust set point	robust nominal	D1	D2	D3	D4	D5	D6	D7	D8	D9	D10	D11	D12	D13	D14	D15	D16	D17	average loss
P_{F1}	−202.61	−314.22	0.0049	0.0049	0.0049	0.0005	0.0049	0.0049	0	0.0050	0.0050	0.0049	0.0047	0.0032	0.0034	0.0071	0.0063	0.0052	0.0049	0.0048	0.0044
P_{F2}	−200	−308.78	0.0048	0.0047	0.0048	0.0047	0	0.0005	0.0047	0.0046	0.0043	0.0024	0.0048	0.0047	0.0047	0.0069	0.0061	0.0050	0.0048	0.0047	0.0043
P_{Si}	−755.36	−866.98	0.0049	0.0090	0	0.0048	0.0001	0.0049	0	0.0047	0.0044	0.0026	0.0047	0.0032	0.0034	0.0071	0.0063	0.0052	0.0056	0.0041	0.0042
P_S	−10441.17	−11476.07	0.0349	0.0627	0	0.0472	0.0162	0.0473	0.0161	0.0341	0.0327	0.0257	0.0341	0.0286	0.0293	0.0415	0.0458	0.0374	0.0392	0.0300	0.0335
Z_{F1}	63.87	52.78	0.0224	0.0044	0.0406	0	0.0399	0.022	0.018	0.0236	0.0226	0.0193	0.0222	0.0209	0.0211	0.0321	0.0292	0.0240	0.0222	0.0226	0.0226
Z_{F2}	65.45	54.16	0.0228	0.0043	0.0415	0.0222	0.0185	0	0.0406	0.0227	0.0224	0.0207	0.0238	0.0232	0.0209	0.0327	0.0297	0.0244	0.0226	0.0230	0.0231

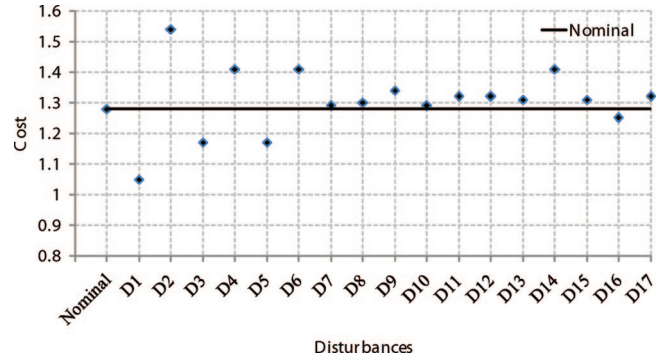

Figure 3. Effect of disturbances (see Table 3) on optimal operation with reduced upper bounds of P_{R1}, P_{R2}, P_{F1}, and P_{F2}.

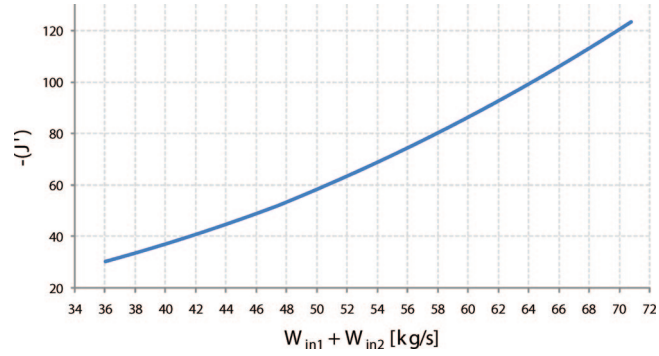

Figure 4. Optimization of the nickel roaster off-gas system with variable feed rate.

are the active constraints at their respective upper bounds. The constraints for P_{R1} and P_{R2} are active because when power requirements are minimized, the net head across a fan is reduced and the pressures at the locations upstream of the fan are increased. As the pressures at the furthermost upperstream location are the largest, they are closer to reaching their constraints. In industrial practice, P_{R1} and P_{R2} are the preferred controlled variables. The constraints for T_{R1} and T_{R2} are active largely due to reduced power consumption from minimizing the amount of water vapor in the system, which in turn takes the two temperatures of the gas coolers to their respective upper bounds. It is noted from Figure 3 that except for disturbance D14, which largely affects the cost as a consequence of the large in-leakage area in the gas cleaning section, the effect of air in-leakage on the cost is small compared to the other disturbances.

4.3.1. Unconstrained Degree of Freedom Selection and Feasibility Analysis. When the two gas flow rates of the roasters are not available for control, 5 degrees of freedom are available. As the 4 active constraints must be implemented to ensure optimal operation,[18] we are left with 1 degree of freedom. It is necessary to find a suitable controlled variable that when kept at its nominal optimum set point leads to near-optimal operation for the disturbances considered in Table 3. Self-optimizing control technology was used to tackle this issue. Table 5 shows the loss results for the various optimization runs, where each one of the candidate controlled variables was kept constant at its nominal optimum, with the constraint variables controlled. For brevity of Table 5, the results for two representive disturbances related to in-leakage area, D7 and D10, are displayed, and the effects of other in-leakage area disturbances are not included.

It can be noticed from Table 5 that although the losses are very small, there is no candidate that gives feasible operation

Table 7. Reoptimization with Variable Feed Rates W_{in1} and W_{in2} as Degrees of Freedom

variable	nominal	maximum	maximum increase at $W_{in1} + W_{in2}$ [kg/s]	comments
ID fan 2 vane position [%]	65.46	100	47.1 (+31%)	$W_{in1} = 23.59$ $W_{in2} = 23.51$
ID fan 1 vane position [%]	63.89	100	47.5 (+32%)	$W_{in1} = 23.90$ $W_{in2} = 23.60$
blower vane position [%]	45.65	100	70.7 (+96%)	$W_{in1} = 35.56$ $W_{in2} = 35.14$ bottleneck

Table 8. Disturbances to the Process at the Maximum Throughput

	disturbance description	nominal	disturbance (Δ)
D1	effective in-leakage area in roaster 1 [m^2]	0.0120	+0.0060 (+50%)
D2	effective in-leakage area in roaster 1 to ESP 1 inlet [m^2]	0.0190	+0.0095 (+50%)
D3	effective in-leakage area in ESP 1 [m^2]	0.0590	+0.0295 (+50%)
D4	effective in-leakage area in roaster 2 [m^2]	0.0110	+0.0055 (+50%)
D5	effective in-leakage area in roaster 2 to ESP 2 inlet [m^2]	0.0530	+0.0265 (+50%)
D6	effective in-leakage area in ESP 2 [m^2]	0.0350	+0.0175 (+50%)
D7	effective in-leakage area from ID fan duct to scrubber inlet [m^2]	0.0820	+0.0410 (+50%)
D8	effective in-leakage area in gas cleaning section [m^2]	0.1300	+0.0650 (+50%)
D9	Effective in-leakage area in blower inlet [m^2]	0.0220	+0.0110 (+50%)
D10	room temperature [K]	273	−30
D11	room temperature [K]	273	+30

for the entire range of disturbances. Nevertheless, the concept of self-optimizing control can still be applied to this process to find a "robust" set point for the remaining degree of freedom using the robust optimization approach discussed in Govatsmark and Skogestad.[21] It consists of a large optimization run over all the disturbances so as to guarantee simultaneous feasibility. The problem to be solved can be formulated as

$$\min_{c_s} \sum_i J(x_i, u_i, d_i)$$

subject to

$$\begin{aligned} &f(x_i, u_i, d_i) = 0 \\ &g(x_i, u_i, d_i) \le 0 \\ &c(x_i, u_i, d_i) = c_s \\ &d_i = d_0 + \Delta d_i \\ &\Delta d_i \in D_d \end{aligned} \tag{3}$$

where f includes all equality constraints in addition to the process model, g are the inequality constraints, c is the candidate controlled variable that needs to be fixed at c_s for all expected disturbances ($\Delta d_i \in D_d$) given by the index i. The objective function is the summation of eq 2 over the entire set of disturbances in Table 3.

This optimization problem was solved for each candidate controlled variable and the results for those that generate feasible operation shown in Table 6 (active constrained variables are included). It can be seen from Table 6 that, among all the variables considered, only six candidate controlled variables give feasible robust operation. The smallest average losses are found for the candidates P_{Si}, P_{F1}, and P_{F2}, and any one of them can be chosen as the self-optimizing variable, but the final choice is dictated by the dynamic performance of the system. It is interesting to note that keeping one of the ID fan vane positions (Z_{F1} and Z_{F2}) constant is also a viable policy, at least at steady state, though the average loss is 4 times larger.

4.4. Production Rate. Two modes of operation are considered:

Mode I: given feed rate. The optimal operation for this mode is considered for fixed inlet gas flow rate of the roaster freeboards, W_{in1} and W_{in2}.

Mode II: maximum throughput. Now we determine the evolution of the static behavior of the system as we allow W_{in1} and W_{in2} to increase. With given prices for the final product, it is optimal, from an economic point of view, to increase the production rate as much as possible because the actual profit of the enterprise increases almost linearly with the feed rate. However, as discussed in detail below, other process constraints result in bottlenecks that prevent this increase above a certain maximum.

Optimization for mode I is presented in the last subsection. For mode II, to find the maximum throughput, the available (maximum) feed rates W_{in1} and W_{in2} are used as degrees of freedom and the process is reoptimized using the revised cost function J':

$$J' = \frac{pK}{\varepsilon\rho C_q}[(P_{F1} - P_{E1})W_{F1} + (P_{F2} - P_{E2})W_{F2} + (P_B - P_S)W_B] - p_F(W_{in1} + W_{in2}) \tag{4}$$

where p_F is the price of feed and the constraints used are $P_{R1} < -1000$ Pa, $P_{R2} < -1000$ Pa, $P_{F1} < -200$ Pa, and $P_{F2} < -200$ Pa.

The results are summarized in Table 7 and the cost as a function of $W_{in1}+W_{in2}$ is shown graphically in Figure 4. It is worth mentioning that the active constraints on each optimization run are the same as per mode I, that is, P_{R1} (upper bound), T_{G1} (upper bound), P_{R2} (upper bound), and T_{G2} (upper bound).

The bottleneck is reached when the blower vane position ($Z_B = 100\%$) saturates after the two ID fan vane positions saturate ($Z_{F1} = 100\%$ and $Z_{F2} = 100\%$), as seen in Table 7. Operation beyond this point is no longer feasible and all available degrees of freedom are used to satisfy the new set of active constraints, P_{R1}, T_{G1}, P_{R2}, T_{G2}, Z_{F1}, Z_{F2}, and Z_B. One may also expect gas out-leakage for feed rates ($W_{in1} + W_{in2}$) larger than 196% of the nominal.

For mode II of operation, the bottleneck is the blower vane position (Z_B), and the optimal production rate should be set such that $Z_B = 100\%$ for maximum throughput ($W_{in1} + W_{in2} = 70.7$ kg/s). However, when disturbances are considered, the maximum throughput changes accordingly. Assume the plant is subject to the disturbances listed in Table 8, then results at the maximum throughput for each disturbance are given in Table 9 and Figure 5. It is noticed that the cost and the maximum throughput do not change much when disturbances upset the

Table 9. Effect of Disturbances on the Maximum Throughput

variable	unit	nominal	D1	D2	D3	D4	D5	D6	D7	D8	D9	D10	D11
P_{R1}	Pa	−1000	−1000	−1000	−1000	−1000	−1000	−1000	−1000	−1000	−1000	−1000	−1000
P_{C1}	Pa	−7407	−7412	−7344	−7277	−7409	−7325	−7298	−7236	−7152	−7324	−7502	−7315
P_{G1}	Pa	−9970	−9977	−9882	−9787	−9973	−9854	−9818	−9731	−9613	−9853	−10102	−9841
T_{G1}	K	643	643	643	643	643	643	643	643	643	643	643	643
P_{E1}	Pa	−13445	−13448	−13402	−13191	−13449	−13284	−13233	−13113	−12949	−13283	−13549	−13343
P_{Si}	Pa	−7397	−7401	−7341	−7070	−7400	−7249	−7203	−7092	−6943	−7248	−7508	−7288
P_S	Pa	−26460	−26462	−26433	−26298	−26462	−26387	−26364	−26309	−25616	−26185	−26515	−26406
P_{R2}	Pa	−1000	−1000	−1000	−1000	−1000	−1000	−1000	−1000	−1000	−1000	−1000	−1000
P_{C2}	Pa	−7249	−7251	−7218	−7070	−7253	−7077	−7172	−7081	−6999	−7167	−7343	−7155
P_{G2}	Pa	−9748	−9751	−9705	−9497	−9754	−9508	−9641	−9514	−9399	−9634	−9881	−9618
T_{G2}	K	643	643	643	643	643	643	643	643	643	643	643	643
P_{E2}	Pa	−13423	−13427	−13363	−13067	−13426	−13308	−13271	−13091	−12928	−13261	−13527	−13321
Z_{F1}	%	100	100	100	100	100	100	100	100	100	100	100	100
Z_{F2}	%	100	100	100	100	100	100	100	100	100	100	100	100
Z_B	%	100	100	100	100	100	100	100	100	100	100	100	100
P_{F1}	Pa	−5301	−5306	−5221	−4828	−5303	−5180	−5142	−5051.45	−4929.18	−5179	−5425	−5178
W_{F1}	kg/s	45.8	45.8	46	47.4	45.8	45.5	45.4	45.2	44.9	45.5	45.6	45.9
P_{F2}	Pa	−5345	−5348	−5299	−5076	−5350	−5133	−5065	−5095	−4972	−5223	−5471	−5222
W_{F2}	kg/s	45.3	45.3	45.2	44.7	45.3	46	46.2	44.7	44.4	45	45.1	45.5
P_B	Pa	31100	31098	31137	31317	31098	31198	31229	31302	32231	31327	31026	31172
W_{w1}	kg/s	4.75	4.71	4.63	4.70	4.75	4.71	4.70	4.68	4.65	4.71	4.31	5.18
W_{w2}	kg/s	4.38	4.38	4.36	4.31	4.35	4.07	4.35	4.31	4.28	4.35	3.92	4.83
cost	−	5.21	5.21	5.22	5.26	5.21	5.24	5.24	5.23	5.37	5.23	5.20	5.23

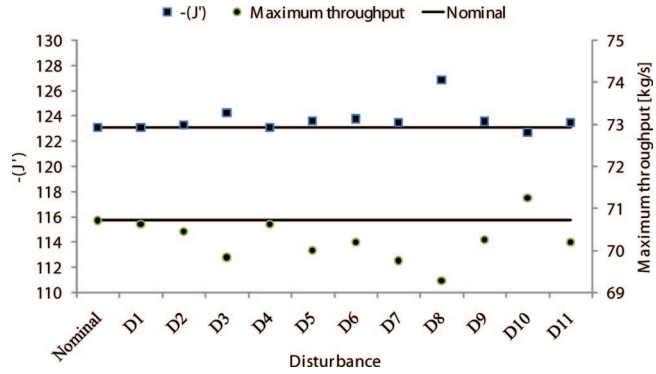

Figure 5. Effect of disturbances (see Table 8) on operation at maximum throughput (mode II).

process at the maximum throughput. This is due to the nature of the disturbances in Table 8 which consist basically of in-leakage effects and have small impact on the cost.

5. Bottom-up Design

In this section, the control configuration for the nickel smelter off-gas system is designed using the Steps 5−8 described in section 3.

5.1. Structure of the Regulatory Control Layer. The main objective of this layer is to provide sufficient quality of control and to enable a trained operator to keep the plant running safely without the need for using higher layers in the control system. The regulatory control layer should be designed such that it is independent of the mode of operation.[23]

One of the primary objectives of the regulatory control layer is to prevent the plant from drifting away from its desired operating point on a short time scale. As pressure dynamics are generally very fast, the drift due to disturbances in these variables is avoided by controlling pressure at selected locations in the plant. Along these lines, the pressures in the roasters, P_{R1} and P_{R2}, are controlled. In mode I, the two ID fan vane positions, Z_{F1} and Z_{F2}, are used as the manipulated variables, as they are easy to measure, reliable, and do not introduce any effective delays in the process. Some delay may exsit in the loops because the manipulations are located far from measurement. Unfortunately, this is unavoidable since the closest manipulated variables, the two cooling water flow rates (W_{w1} and W_{w2}), do not affect P_{R1} and P_{R2}. In mode II, Z_{F1} and Z_{F2} are not available for control, and therefore, P_{R1} and P_{R2} are controlled by manipulating the two feed rates to the process, W_{in1} and W_{in2}. This choice can avoid the delay problem encountered in mode I and produces faster responses. Both configurations ensure smooth operation of the units downstream the roasters and that active constraints be controlled.

Temperature measurement is fast and reliable, and hence temperature loops are frequently closed to avoid drift. The temperatures T_{G1} and T_{G2} should be controlled as they affect process operation and the cooling water flow rates, W_{w1} and W_{w2}, are used as the manipulated varables. The gains from the

Table 11. Tuning Parameters for the Roaster Off-Gas System (Modes I and II)

MV	CV	K_c	τ_I	τ_D	comment
Z_{F1}	P_{R1}	0.0017% /Pa	0.374 s	1.102 s	mode I
Z_{F2}	P_{R2}	0.0017% /Pa	0.374 s	1.102 s	mode I
Z_B	P_{Si}	0.0020% /Pa	0.479 s	0.985 s	mode I
W_{in1}	P_{R1}	0.0005 (kg/s)/Pa	0.632 s	−	mode II
W_{in2}	P_{R2}	0.0005 (kg/s)/Pa	0.632 s	−	mode II
W_{w1}	T_{G1}	0.0129 (kg/s)/K	0.691 s	−	mode I and II
W_{w2}	T_{G2}	0.0129 (kg/s)/K	0.691 s	−	mode I and II

Table 10. Structure of the Regulatory Layer for the Roaster Off-Gas System (Mode I and Mode II)

loop no.	MV[a]	CV[b]	comment
R1	ID fan 1 vane position (Z_{F1})	roaster 1 pressure (P_{R1})	mode I
R2	ID fan 2 vane position (Z_{F2})	roaster 2 pressure (P_{R2})	mode I
R1a	flow rate to roaster 1 freeboard (W_{in1})	roaster 1 pressure (P_{R1})	mode II
R2a	flow rate to roaster 2 freeboard (W_{in2})	roaster 2 pressure (P_{R2})	mode II
R3	cooling water to gas cooler 1 (W_{w1})	gas cooler 1 temperature (T_{G1})	mode I and II
R4	cooling water to gas cooler 2 (W_{w2})	gas cooler 2 temperature (T_{G2})	mode I and II

[a] MV stands for manipulated variable. [b] CV stands for controlled variable.

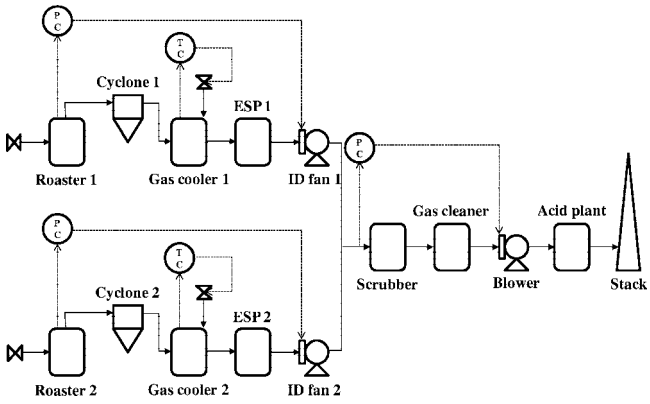

Figure 6. Control configuration for mode I of operation.

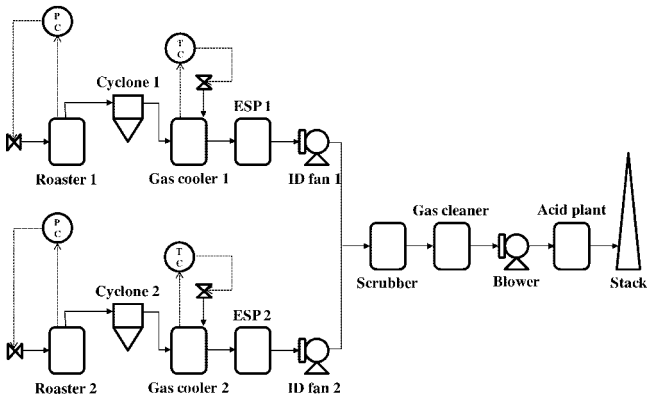

Figure 7. Control configuration for mode II of operation.

cooling water flow-rates to the temperatures are large, ensuring effective control of the temperatures without delay. It is also assumed that the flow of water does never saturate. T_{G1} and T_{G2} are active constraints and need to be controlled.

Table 10 summarizes the structure of the proposed regulatory control layer.

5.2. Structure of the Supervisory Control Layer. The supervisory control layer is to keep the active constraints and unconstrained (self-optimizing) controlled variables at their constant optimum set points. For the unconstrained controlled variables, the scrubber inlet pressure P_{Si} was selected in mode I to be controlled using the blower vane position (Z_B). In mode II, the two ID fans vane positions and the blower vane position were kept fully open, i.e., $Z_{F1} = 100\%$, $Z_{F2} = 100\%$, and $Z_B = 100\%$. The strategies favor optimal economic performance with minimal losses. The production rate was manipulated using the two feed rates to the roasters, W_{in1} and W_{in2}. It was fixed in mode I and adjusted to give the desired maximum throughput in mode II.

Switching from mode I to mode II may be accomplished through the following logic steps: (1) Break the loop between P_{R1} and Z_{F1}, and P_{R2} and Z_{F2}. Fix $Z_{F1} = 100\%$ and $Z_{F2} = 100\%$. (2) Use W_{in1} to control P_{R1} and W_{in2} to control P_{R2} (to ensure active constraint control). (3) Break the loop between P_{Si} and Z_B and fix $Z_B = 100\%$. (4) The loops $T_{G1}-W_{w1}$ and $T_{G2}-W_{w2}$ remain the same. (5) Tune the loops using the parameters listed in Table 11. Note that only the loops $P_{R1}-W_{in1}$ and $P_{R2}-W_{in2}$ need to be retuned.

The final configurations for both modes of operation are shown in Figure 6 and Figure 7.

Since the design discribed above can take care of important disturbances (self-optimizing control structure) with acceptable loss, online optimization is not needed.

5.3. Validation of the Proposed Control Structures. Dynamic simulations were performed to validate the proposed control structure for various disturbances (Table 3). The control loops were tuned one at a time in a sequential manner, starting with the fastest ones. SIMC tuning rules[23] were used to design the PI/PID controllers and the controllers parameters - gain K_c, integral time τ_I and derivative time τ_D - are given in Table 11.

Figure 8 illustrates the output responses of roaster 1 freeboard pressure at various disturbances in mode I of operation. For the sake of compactness, only the most relevant disturbances

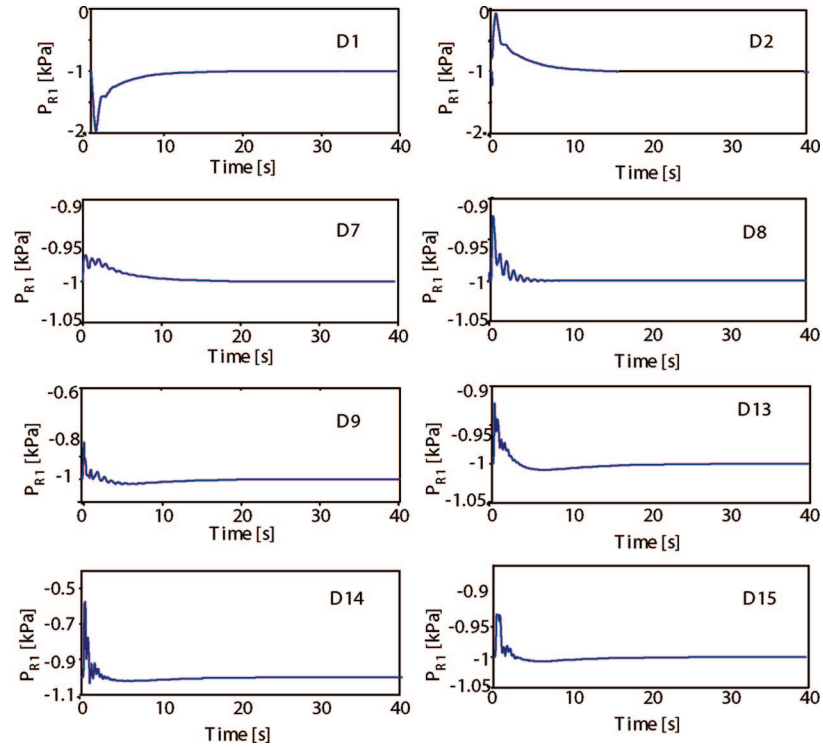

Figure 8. Response of the roaster 1 freeboard pressure to various disturbances in mode I of operation.

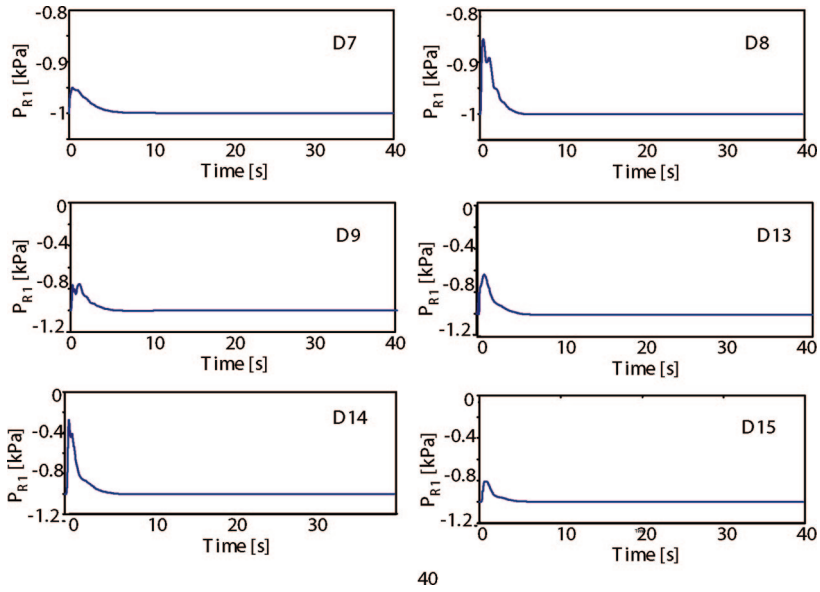

Figure 9. Response of the roaster 1 freeboard pressure to various disturbances in mode II of operation.

Table 12. Summary of the Robust Optimization

variable	unit	original after Shang et al.[13]	nominal optimum	robust P_{Si}	robust P_S	robust Z_{F1}	robust Z_{F2}	robust P_{F1}	robust P_{F2}
P_{R1}	Pa	1259	−1000	−1000	−1000	−1000	−1000	−1000	−1000
P_{C1}	Pa	−361	−2664	−2661	−2661	−2661	−2661	−2661	−2661
P_{G1}	Pa	−1009	−3329	−3326	−3326	−3326	−3326	−3326	−3326
T_{G1}	K	633	643	643	643	643	643	643	643
P_{E1}	Pa	−1879	−4229	−4225	−4225	−4225	−4225	−4225	−4225
P_{Si}	Pa	371	−755	−867	−1660	−1310	−1320	−867	−864
P_S	Pa	−8587	−10441	−10572	−11476	−11081	−11093	−10572	−10569
P_{R2}	Pa	1311	−1000	−1000	−1000	−1000	−1000	−1000	−1000
T_{R2}	K	972	964	964	964	964	964	964	964
P_{C2}	Pa	−308	−2658	−2658	−2658	−2658	−2658	−2658	−2658
P_{G2}	Pa	−956	−3321	−3321	−3321	−3321	−3321	−3321	−3321
T_{G2}	K	623	643	643	643	643	643	643	643
P_{E2}	Pa	−1879	−4306	−4306	−4306	−4306	−4306	−4306	−4306
Z_{F1}	%	40	63.9	61.6	45.8	52.8	52.6	61.6	61.7
Z_{F2}	%	40	65.5	63.2	47.4	54.4	54.2	63.2	63.3
Z_B	%	40	45.7	46	48.2	47.2	47.3	46	46
P_{F1}	Pa	873	−203	−314	−1107	−757	−767	−314	−311
P_{F2}	Pa	873	−200	−312	−1104	−754	−765	−312	−309
P_B	Pa	15054	16332	16376	16648	16535	16538	16376	16375
W_{w1}	kg/s	2.50	2.32	2.32	2.32	2.32	2.32	2.32	2.32
W_{w2}	kg/s	2.50	2.15	2.15	2.15	2.15	2.15	2.15	2.15
cost		1.01	1.28	1.29	1.32	1.31	1.31	1.29	1.29

were considered. For mode I of operation, the responses at the disturbances D1, D2, D7, D8, and D13-D15 are displayed. It can be seen that the proposed control design can effectively reject the disturbances and the output returns back to the setpoint quickly when disturbances occur (very short settling time, 20 s at most). When a large change in feed flow rate occurs, as shown for the cases of D1 and D2 in Figure 8, the controller can maintain a negative freeboard pressure and drive the pressure back to the setpoint. It is also observed that the effect of a sudden "burst" in in-leakage spots around the system is promptly addressed by the control scheme. The output responses of other variables under the disturbances were evaluated and the satisfactory responses were observed. For brevity of description, they are not displayed in the paper.

For mode II of operation, effectiveness of the proposed control design under the disturbances D7−D9 and D13−D15 were evaluated since W_{in1} and W_{in2} are manipulated variables and assumed perfectly adjustable. As before, the output responses of all the important variables were tested but only the responses of the roaster 1 freeboard pressure are displayed in Figure 9. It can be observed that the proposed controlled structure exhibits the effective disturbance rejection capability at maximum throughput with fast output responses characterized by small settling time.

6. Discussion

This paper has discussed the design of a control structure for a nickel smelter roaster off-gas system. The objective was to minimize the (energy) cost of the process by keeping economic variables at their optimal set points while providing stable and smooth operation at either a fixed feed flow rate or at maximum throughput capacity. It is also paramount to avoid positive pressures across the system to prevent out-leakage of hazardous gas (SO_2) to the atmosphere.

Results of this work provide validation of the current industrial practice of "controlling" the farthermost pressures in the roaster freeboards (P_{R1} and P_{R2} are active constraints at their upper bounds), which ensure near optimal operation if running the process at the proper optimum operating point. Moreover,

we show that the temperatures exiting the gas coolers (T_{G1} and T_{G2}) should be kept at their upper bounds to minimize the amount of water vapor in the system. This is an advantage since less water is consumed by the process.

With fixed inlet gas flow rate to the roasters (mode I of operation), there is still one degree of freedom left for optimization and it was used to improve process economics. The robust optimization analysis yielded as possible candidates (those with smaller losses) one of the two ID fans outlet pressures (P_{F1} or P_{F2}), or the scrubber inlet pressure (P_{Si}). However, the issue of which nominal condition the plant should operate must be considered since robust optimization yields different set points for the decision variables. This is a function of the selected self-optimizing variable, as seen in Table 12, and any one of the six variables which could be chosen, since they all result in acceptable loss. The scrubber inlet pressure (P_{Si}) was subsequently selected because it was found through dynamic simulation runs that P_{Si} gives better dynamic performance than the other candidates. It can be also noticed from Table 12 that though having the lowest cost, the original configuration as given by the operating conditions after Shang et al.[13] is not feasible with positive pressures in the roasters freeboards. The nominal optimum as given in Table 12 and calculated in Table 5 is not the operating point of choice, for it renders infeasible operation under the self-optimizing regime when disturbances occur (see Table 5).

As more feed rate to the plant (mode II of operation) is required, the bottleneck of the process is the blower vane position, Z_B, corresponding to a total throughput of $W_{in1} + W_{in2} = 70.7$ kg/s. The two roaster lines operate in parallel and increasing throughput is accomplished by simultaneous manipulation of the feed rates to both lines. At maximum capacity, the variables to be controlled are the active constraints, P_{R1}, T_{G1}, P_{R2}, and T_{G2}, at their respective upper bounds, and Z_{F1}, Z_{F2}, and also Z_B must be kept fully open. Results of this work indicate that at steady-state the off-gas system can almost double its capacity and still operate satisfactorily.

When it comes to the bottom-up design, at the regulatory control layer the system needs to be "stabilized". At this layer, the pressures in the roaster freeboards (P_{R1} and P_{R2}) were selected as the controlled variables to guarantee smooth operation of the downstream units. In addition, temperatures in the gas coolers (T_{G1} and T_{G2}) were controlled since these temperatures largely affect process operation and are, therefore, also active constraints as economic variables.

As for the supervisory control layer, which has the important task of keeping the active constraints and unconstrained variables at their optimum set points, we controlled the scrubber inlet pressure (P_{Si}) in mode I of operation and simply kept the two fans and the blower vanes fully open in mode II.

Both the regulatory and supervisory designs generate very simple control configurations. Simulations show they are very effective in rejecting disturbances and tracking set points.

7. Conclusion

A systematic plantwide procedure was applied to design a control structure for a smelter roaster off-gas system. The study validates some of the industrial practices in pressure control of the system and provides a useful guideline for further improvement. Simulation results indicate that the control structures obtained from the plantwide procedure can reject the disturbances effectively and quickly and maintain negative pressure in the system and, therefore, minimize SO_2 out-leakage. This work shows that safe operation in combination with optimized cost of such units is possible and relatively easy to achieve.

The results of such analysis can be extended with few adjustments to other off-gas units in different metallurgic processes as well as gas cleaning systems in other industrial sectors.

Acknowledgment

The authors gratefully acknowledge the financial support provided by Centre for Excellence in Mining Innovation (CEMI).

Literature Cited

(1) Ciccone, A.; Storbeck, J. Fugitive SO_2 and Particulate Emissions from a Smelter Complex. Presented at Air and Waste Management Association's Annual Meeting and Exhibition, June 1997, Toronto, Canada.

(2) Chan, W. H.; Vet, R. J.; Ro, C.; Tang, A. J. S.; Lusis, M. A. Impact of Inco smelter emissions on wet and dry deposition in the Sudbury area. *Atmos. Environ.* **1984**, *18*, 1001.

(3) Chan, W. H.; Vet, R. J.; Ro, C.; Tang, A. J. S.; Lusis, M. A. Long-term precipitation quality and wet deposition fields in the Sudbury basin. *Atmos. Environ.* **1984**, *18*, 1175.

(4) Gunn, J.; Keller, W.; Negusanti, J.; Potvin, R.; Beckett, P.; Winterhalder, K. Ecosystem recovery after emission reductions: Sudbury, Canada. *Water, Air Soil Pollut.* **1995**, *85*, 1783.

(5) Sudbury, M. P.; Crawford, G. A. Sulphur abatement at Ontario operations of Falconbridge Limited. Air and Waste Management Association's Annual Meeting and Exhibition, June 1989, Anaheim, CA.

(6) Bekker, J. G.; Craig, I. K.; Pistorius, P. C. Modeling and simulation of an electric arc furnace process. *Iron Steel Inst. Jpn. Int.* **1999**, *39*, 23.

(7) Zietsman, J. H.; Pistorius, P. C. Modeling of an ilmenite-smelting DC arc furnace process. *Miner. Eng.* **2006**, *19*, 262.

(8) Cain, S. L.; Budman, H. M.; Pritzker, M. On-line estimation of matte grade in a copper smelter. *Can. J. Chem. Eng.* **1996**, *74*, 993.

(9) Ronan, P.; Budman, H. M.; Pritzker, M. Pseudoequilibrium model-based estimator of matte grade in a copper smelter. *Ind. Eng. Chem. Res.* **1997**, *36*, 112.

(10) Bekker, J. G. Modelling and control of an electric arc furnace off-gas process. Master Thesis. University of Pretoria: South Africa, 1999.

(11) Bekker, J. G.; Craig, I. K.; Pistorius, P. C. Model predictive control of an electric arc furnace off-gas process. *Control Eng. Pract.* **2000**, *8*, 445.

(12) Marcuson, S. W. SO_2 Abatement from Copper Smelting Operations: A 35 Years Perspective. 55th Canadian Chemical Engineering Conference, October 2005, Toronto, Canada.

(13) Shang, H.; Mehta, B.; Thwaites, P.; Ryan, L.; Nelson, P. Dynamic modelling of an industrial roaster off-gas system in a nickel smelter. *Ind. Eng. Chem. Res.* **2007**, *46*, 5371.

(14) Skogestad, S. Control structure design for complete chemical plants. *Comput. Chem. Eng.* **2004**, *28*, 219.

(15) McKague, A. L.; Norman, G. E.; Jackson, J. F. Falconbridge nickel mines limited - New smelting process. *Can. Inst. Min., Metall., Petrol. Bull* **1980**, *73*, 132.

(16) Araujo, A.; Govatsmark, M.; Skogestad, S. Application of plantwide control to the HDA process. I - Steady-state optimization and self-optimizing control. *Control Eng. Pract.* **2007**, *15*, 1222.

(17) Araujo, A.; Hori, E. S.; Skogestad, S. Application of plantwide control to the HDA process. II - regulatory control. *Ind. Eng. Chem. Res.* **2007**, *6*, 5159.

(18) Maarleveld, A.; Rijnsdorp, J. E. Constraint control on distillation columns. *Automatica* **1970**, *6*, 51.

(19) Jorgensen, R. *Fan Engineering*; Buffalo Forge Company: Buffalo, NY, 1983.

(20) Shang, H.; Thwaites, P.; Ryan, L.; Nelson, P. Comparison of Different Control Methods for an Industrial Nickel Smelter Roaster off-Gas System. 12th IFAC Symposium on Automation in Mining, Mineral and Metal Processing, IFAC MMM'07, August 2007, Quebec City, Canada.

(21) Govatsmark, M. S.; Skogestad, S. Selection of controlled variables and robust set points. *Ind. Eng. Chem. Res.* **2005**, *44*, 2207.

(22) Skogestad, S.; Postlethwaite, I. *Multivariable Feedback Control: Analysis and Design*; John Wiley and Sons: Chichester, UK, 2005.

(23) Skogestad, S. Simple Analytic Rules for Model Reduction and PID Controller Tuning. *Model., Ident. Control* **2004**, *25*, 85.

Received for review November 14, 2007
Revised manuscript received January 6, 2009
Accepted January 7, 2009

IE800254S